https://doi.org/10.1016/j.ceramint.2021.12.246

Polymer Derived SiBCN(O) Ceramics with Tunable Element Content

Bijie Wang# [1, 3], Yujie Song#* [1, 3], Xiao Zhang[2], Ke Chen[1, 3], Ming Liu[4], Xiao Hu[5], Liu He[1, 3], and Qing Huang[1, 3]

1. Engineering Laboratory of Advanced Energy Materials, Ningbo Institute of Materials Technology & Engineering, Chinese Academy of Sciences, Ningbo 315201, China.
2. Department of Mechanical Engineering, The Hong Kong Polytechnic University, Hung Hom, Kowloon, Hong Kong SAR, China.
3. Qianwan Institute of CNiTECH, Ningbo 315336, China.
4. Harbin Institute of Technology, 92 West Dazhi Street, Nan Gang District, Harbin, Heilongjiang, 150001, China.
5. School of Materials Science and Engineering, Nanyang Technological University, Block N4.1, Nanyang Avenue, 639798, Singapore.

# These authors contributed equally to this article

Corresponding author: songyujie@nimte.ac.cn

Abstract

SiBCN ceramics have excellent high-temperature stability and anti-oxidation properties, and they are candidates for materials used at extreme conditions. In this paper, amorphous SiBCN(O) ceramics were obtained through pyrolysis of cross-linked polyborosilazanes. The element content could be readily tuned through adjusting the structures of polymer precursors. The cerminization process and microstructure evolution process were systematically investigated. The SiBCN(O) ceramics remain amorphous

before 1400 °C. The carbothermal reduction was suppressed because of the presence of boron. The SiBCN(O) ceramics showed 95.7% and 99.2% carbon residual in argon and air at 1600 °C, indicating high-temperature stability and good anti-oxidation properties. These SiBCN(O) precursors/ceramics could be potentially used in composites or protective coatings for harsh environments.

Keywords

SiBCN(O); Polymer Derived Ceramics; Oxidation; Microstructure

1. Introduction

Si-based amorphous polymer-derived ceramics (PDCs) have advantages over traditional ceramics, such as facile tuning of element content through adjusting the structure of preceramic polymers, low sintering temperature, and easy processing.[1-3]. It has changed the way of preparing ceramic materials from inorganic powder at high temperature, and it is ideal for the design of ceramics through precise control of element content.

There are two main stages in the manufacture of PDCs: the synthesis of preceramic polymers and the conversion of polymers to ceramics[4-6] The composition and microstructure of the ceramics can be readily controlled and adjusted by selecting the appropriate preceramic polymers and controlling the sintering conditions, thus obtaining ceramics with targeted properties. For instance, amorphous SiC, SiCO, SiCN, SiBCN and SiBCO ceramics can be obtained from polycarbosilane[7, 8], polysiloxane[9, 10],

polysilazane[11]. polyborosilazane[2, 12-14] and poly(borosiloxane)[15] after heat treatment at about 1000 °C, and the microstructure and properties could be further tuned through introduction of hetero-elements to preceramic polymers.

Polyborosilazane (PBCS) is a class of important precursor for ceramics applied under extreme conditions and it could be used in coatings, ceramic fibers, and composites because of the outstanding high-temperature stability, remarkable oxidation resistance, easy processing, creep resistance properties and designable precursor structure[16]. Compared with the binary and ternary ceramic matrixes, the ceramics derived from PBCS (SiBCN ceramics) have higher temperature resistance. Takamizawa et al. [17] firstly reported a method for synthesizing a multi-component ceramic precursor of the Si-B-C-N system in 1985. They mixed polysilazane and organoboron compounds containing Si-C and BN bond, and then post-cured the preceramic polymers in an inert atmosphere at 500 °C to undergo polycondensation reaction, forming a cross-linked polymer containing Si, B, C, and N elements. R. Riedel [18] reported SiCN ceramic ceramics that can be used at 1600 °C. Mülle [19, 20] synthesized SiBCN quaternary ceramics that can withstand 2000 °C. Yu et al. [21] found that boron can effectively inhibit the decomposition of ceramics at 1400 – 1600 °C. With the increase of boron content, SiBCN ceramics have a higher carbon residue rate. The amorphous structure of boron has an inhibitory effect on the decomposition of silicon nitride and ceramic crystallization, and causes more dynamic constraints on the migration of atoms in the structure in the ceramic network[22], but in a boron-rich system, the excess boron would contributes to crystallization [23]. However, the normally adopted single-source polymer precursor is sensitive to air and the element

content is fixed for specific structure. Developing novel precursor systems with tunable structure and element content could contribute to deep understanding of structure-microstructure evolution-property relationship.

In our previous research, we used polyvinyl boron-containing silazane as crosslinker to react with polysilazane in the air, and obtained cross-linked polyborosilazane (CPBCSs) with different structures.[24] The polyborosilizanes showed good thermal stability and high char yields, which indicated potential applications in ceramic precursors. This method also offers structure and element tunning in precursors design. In the present work, we investigated the ceraminization process and microstructure evolution of SiBCN(O) ceramics, and found that the SiBCN(O) ceramics remained amorphous before 1400 °C and showed excellent thermal stability in both argon and air. The low viscosity of polyborosilizane mixtures before curing enables easy processing, and they could be potentially used for composites and protective coatings under harsh environments. Besides, the storage stability of the two-component precursor at ambient environment is better than that of previously studied single-source precursor, and the element content could be readily tuned through adjusting the ratio of the raw materials used.

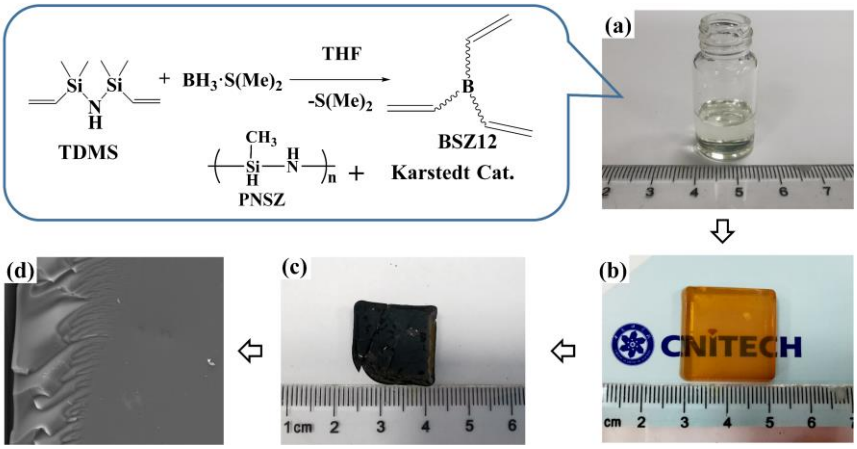

Figure 1 Optical picture of (a) CPBCS precursor; (b) CPBCS precursor after cured at 300 °C; (c) CPBCS precursor after pyrolysis at 1200 °C; (d) SEM of derived ceramics at 1200 °C.

2. Material and methods

2.1. Preparation of ceramic materials

Tetrahydrofuran (THF), Borane-methyl sulfide complex (BDMS, 2.0 M solution in THF), 1,1,3,3-Tetramethyl-1,3-divinyldisilazane (TMDS) and Karstedt Catalyst Solution (Pt: ~2% Xylene solution) were purchased from Aladdin Reagent Co., Ltd.(Shanghai, China). Poly[imino(methylsilylene)] (PNSZ) was purchased from Guangzhou Winhigh Chemical & Technology Co., Ltd.(Guangzhou, China).

The synthesis of polyborosilizanes was described in our previous work.[24] The multifunctional boron hybrid silazane monomers (BSZ12) was synthesized through the hydroboration reaction between TMDS and BDMS. TMDS was dissolved in anhydrous THF and BDMS was added to the TMDS solution drop by drop under the protection of argon at 0 °C. The mixture was stirred overnight at room temperature to obtain the BSZ12 intermediate. THF was removed by reduced pressure distillation.

CPBCS samples with different boron contents were prepared with different Si-H/C=C ratios by mixing appropriate amount of PNSZ, BSZ12 and Karstedt Catalyst, and the formulations are shown in Table 1. The polyborosilazane samples were cured at 100 °C in air till proper viscosity was achieved and then cured at 300 °C for 2 h under argon flow. Afterward, the cured products were pyrolyzed under an argon atmosphere at temperatures above 1000 °C for 2 h to obtain SiBCN(O) ceramics.

Table 1 Ingredient ratio of CPBCS with BSZ12 and PNSZ

Sample	BSZ12 (g)	PNSZ (g)	Molar ratio(Si-H/C=C)
CPBCS10-1	1.2962	4.000	10-1
CPBCS5-1	2.5924	4.000	5-1
CPBCS3-1	3.2192	3.000	3-1

2.2. Characterization

Thermogravimetry-mass spectrometry (TG-MS) was recorded by NETZSCH STA449F3 (STA, Germany) at a heating rate of 10 °C/min in argon and air atmosphere.

Raman spectra was performed inside a Confocal Raman Microscope (Renishaw inVia Reflex, England). Excitation light energy were recorded 2.71 eV, excitation wavelength was recorded 532.4nm and the scan time were recorded from 4 to 32s.

The Fourier transform infrared (FT-IR) spectra was performed inside a Nicolet Avatar 360 (America) spectrometer using KBr disks. Spectra were recorded from 400 to 4000 cm^{-1} with 32 scans.

The oxygen content and nitrogen content were determined by a LECO ON836 (Germany), the carbon content was determined by LECO CS600(Germany), The hydrogen content was determined by an organic element analyzer (Elementar, Germany), and the boron content was determined by an ICP-OES (SPECTRO ARCOS II, Germany). The silicon content was calculated by subtraction the mass percentage of other elements.

X-ray diffraction pattern was performed inside a D8 ADVANCE (German). The test conditions were recorded with Cu-K, 40 kV/100 mA, 5°/min, and 10 ~ 90°.

X-ray photoelectron spectroscopy analysis was performed inside an AXIS SUPRA (England) to determine the chemical bonds evolution.

Micro morphology was performed on high angle annular dark field (HAADF), high resolution TEM (HRTEM) and selected-area electron diffraction (SAED) techniques inside an Tecnai F20 (America).

3. Results and Discussions

3.1. Ceraminization process of CPBCSs

CPBCS5-1 was selected for investigation on ceraminization process. FTIR spectrum in Figure 2(a) showed the ceraminization process of CPBCS 5-1 in argon. The peaks appeared at 2132 cm^{-1} (Si-H stretching) and 3400 cm^{-1} (N-H stretching) at 200 °C demonstrated the CPBCSs had not fully cured. The stretching peaks of Si-H and N-H bonds disappeared after 400 °C treatment because of hydrosilylation and dehydrogenation coupling occurred[25, 26]. Attenuated peaks of $-CH_3$ / $-CH_2$ (2872cm^{-1}) and $Si-CH_3$ (1350 cm^{-1}) indicated that the organic groups underwent cleavage and escaped from the precursors from 400 °C to 800 °C. After heat-treatment at 1000 °C, there was almost no organic groups detected, indicating the CPBCS was fully converted into SiBCN(O) ceramics.

Figure 2(b) showed the curves of TG-MS in argon atmosphere. The weight loss of CPBCSs in the pyrolysis process was divided into two parts, 40 °C-300 °C and 300 °C - 800 °C. The weight loss before 300 °C was mainly due to the escape of small molecules while the weight loss after 300 °C was due to cleavage and escape of organic groups, which could be verified by NH_3, CH_4, $H_2C=CH_2$, and methylsilanes gases detected by MS in this range. It has been reported that ammonia evolution of the polysilazane-related

polymer occurs before 500 °C due to transamination reaction[27]. Therefore, the slope between 299 and 498 °C in MS spectra (m/z = 16) is attributed to ammonia evolution and ammonia evolution shows an obvious maximum peak at 488 °C. Pyrolysis of carbon chains evolution appears between 249 and 706 °C. $H_2C{=}CH_2$ evolution (m/z = 28) appears between 309 and 702 °C with maximum at 561 °C. Between 292 and 693 °C, the detected ions, such as $[MeSiH]^+$ (m/z = 44) were typical of a mixture of methylsilanes. The broad peak (m/z = 16) between 639 and 707 °C is attributed to release of methane, corresponding the mineralization step[28]. Between 1550 and 1600 °C, SiO (m/z = 44), and CO / N_2 (m/z = 16, 28) was detected, which was released during the carbothermal reduction reaction and the decomposition of Si_3N_4[29, 30]. Chemical reactions which may occur during pyrolyzed between 1550 and 1600 °C are displayed in the following equations.

$$SiO_2 + 3C \rightarrow SiC + 2CO \qquad (1)$$

$$2SiO_2(s) + SiC(s) \rightarrow 3SiO(g) + CO(g) \qquad (2)$$

$$Si_3N_4 + 3C \rightarrow 3SiC + 2N_2(g) \qquad (3)$$

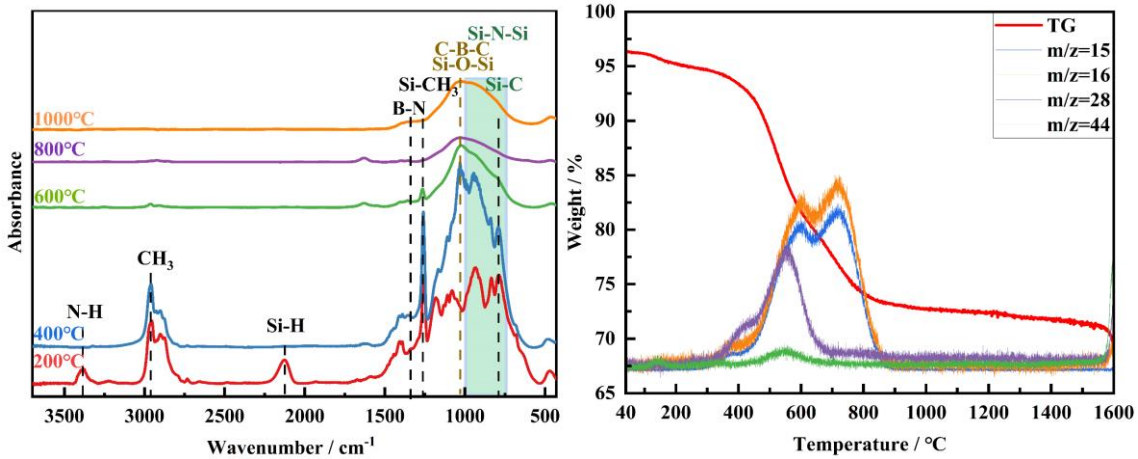

Figure 2 (a)FT-IR spectrum of CPBCS 5-1 samples treated at different temperatures; (b) TG-MS curves of CPBCS 5-1 in argon.

3.2. Microstructure evolution of SiBCN(O) ceramics

Figure 3(a) shows the FTIR spectra of SiBCN(O) ceramics which were prepared through pyrolyzing above 1000 °C. The intensity of Si-O (1022 - 1140 cm^{-1}) and B-C-B (1096 cm^{-1}) peaks were reduced with pyrolysis temperature while the intensity of Si-C and Si–N (824-955 cm^{-1}) bonds increased with pyrolysis temperature. The broad absorption band from 500 to 1100 cm^{-1} suggested the existence of SiC_xN_{4-x} and/or SiC_xO_{4-x} (x=0-4) tetrahedral units[31]. When the pyrolysis temperature exceeded 1200 °C, the covalent bonds in amorphous SiBCN(O) rearranged and redistributed, which led to the presence of Si–O–Si (1090 cm^{-1}) bond and sharp absorption peaks of Si–C and Si–N bonds. The Si-O-Si peak at 1096 cm^{-1} gradually decreased and disappeared after 1400 °C, which is attributed to the thermal decomposition of the C-B-C bonds and carbothermal reduction of the Si-O bonds.

Figure 3(b) shows the Raman spectra of SiBCN(O) ceramics. The peak at 1346 cm^{-1} (D band) is the absorption peak of the amorphous free carbon structure, and the peak at 1594 cm^{-1} (G band) is the absorption peak of the graphite structure and corresponds to the in-plane bond stretching mode E_{2g} of the sp^2 C–C bond[32, 33]. The characteristic peaks at 2950 cm^{-1} (G′ band, nanocrystalline graphite induced band) and 2692 cm^{-1} (D′ band, disorder induced band) appeared after at the SiBCN(O) ceramics were pyrolyzed at 1200 °C, as the second-order spectra of crystalline graphite, demonstrating local deformation of the graphite lattice caused by the finite size of the nanocrystals produced

the selective fracture[33]. The crystal structure of boron atoms is similar to carbon defects, which reduced the in-plane correlation and leading to enhancement of the G′ band and D' band. An obvious characteristic peak appears at 796 cm-1, and the formation of SiC crystals has reached a certain order of magnitude when the ceramic is ablated at 1800 °C, which can be attributed to the TO band of β-SiC[34, 35] or the LO band of 6H–SiC[36].

Figure 3(c) shows the XRD patterns of SiBCN(O) ceramics pyrolyzed at different temperatures. The SiBCN(O) ceramics were amorphous and showed no obvious crystallization peak before 1400 °C. The incorporation of boron contributed to disorder of the ceramic structure, thereby inhibiting the crystallization of SiC. Crystalline peaks of β-SiC, which were located at 35.7°, 41.4°, 60.0°, 71.8° and 75.5°, can be observed at 1600 °C. A peak at 33.7°, which could be attributed to SiC stacking faults.[37] And these defects were caused by the inconsistent orientation of the SiC crystals produced during the ceramic cracking process[38]. The crystalline of SiBCN(O) ceramics was incomplete, which could be concluded in comparison with that of SiBCN(O) ceramic pyrolyzed at 1800 °C. A broad peak around 22° was attributed to high cristobalite peak, indicating that the ceramics oxidation mechanism is mainly active oxidation during ablation[39, 40]. and the appearance of a weak BN(C) peak demonstrated that the addition of boron suppressed the carbothermal reduction till 1600 °C. The SiC grain size in samples pyrolyzed above 1400 °C were calculated by Scherer equation:

$$D=K\lambda / \beta \cos(\theta)$$

where β is the line broadening at half the maximum intensity (FWHM), after subtracting the instrumental line broadening, in radians, θ is the scattering angle in radians, and λ is

the X-ray wavelength, which takes a value 0.15046 nm of Cu tube radiation. *K* is a constant, which normally takes a value of 0.89, and *D* is the dimension of the volume-averaged crystallites, namely grain size.

The grain sizes of SiC of SiBCN(O)5-1 pyrolyzed at 1400 °C, 1600 °C and 1800 °C are 2.4 nm, 16.4 nm, and 75.0 nm, respectively. Heat treatment in the temperature range between 1600 and 1800 °C leads to a rapid thermally activated crystallization process, contributing to SiC crystal growth.

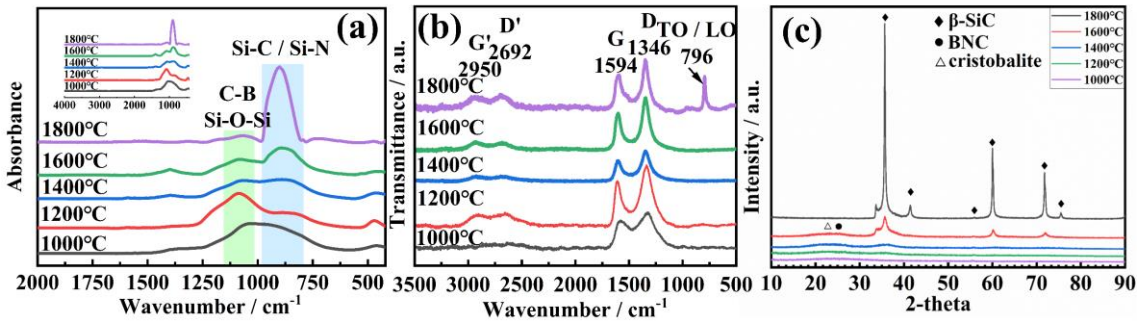

Figure 3 (a) The FT-IR spectra of SiBCN(O) ceramics pyrolyzed from 1000 °C to 1800°C in argon; (b) Raman spectra of SiBCN(O) ceramics heated from 1000 °C to 1800°C in argon.; (c) XRD patterns of SiBCN(O) ceramic pyrolyzed at different high temperature.

The chemical bonds evolution was adopted to determine the chemical composition of the oxide scale. Figure 4 shows the XPS spectra of SiBCN(O) ceramics. For B 1s fitting curves, three types of chemical bonds were detected, namely BNO (189.55 ± 0.05 eV), B_4C (186.88 eV) and BO (188.10 eV). When the SiBCN(O) ceramic was pyrolyzed at 1400 °C, the BNO was partially transformed into B_4C,(Figure 4,(c)) and further pyrolyzing lead to structure rearrangement, forming B-O bond.(Figure 4 (d)) The B-O structure will be continuously evaporated and finally fully disappeared at 1800 °C.(Figure 4 (e)) For N 1s fitting curves, four types of chemical bonds were detected, namely SiN (396.80 ± 0.1 eV), NC (395.40 ± 0.1 eV), BNO (398.55 ± 0.05 eV) and SiNO (398.50

eV). Before 1200 °C, (Figure 4 (f) and (g)), the B-N-O bond was weak due to low boron content. Pyrolyzing precursors at 1400 °C led to C-N bond cleavage and the rearrangement with boron atoms to form B-N-O bonds, making B-N-O signal more significant. (Figure 4, (h)) Presumably, oxygen was combined with the BN structure and formed an amorphous structure, so that the BN phase cannot be significantly observed in XRD patterns. When the pyrolyzing temperature was 1800 °C, only the peak of SiNOx, SiO_2 and SiC phases remain. For Si 2p fitting curves, only two types of chemical bond were detected, namely SiC and SiO. The main content of ceramics is SiC (100.5 ± 0.5 eV). When the temperature is heated to 1000 °C (k), there are a small amount of Si-O bonds (101.10 eV) in addition to SiC bonds. As the heating temperature increases, the bonding of Si-O bonds becomes stronger, and SiO_2 (98.7 ± 0.3 eV) is gradually formed.

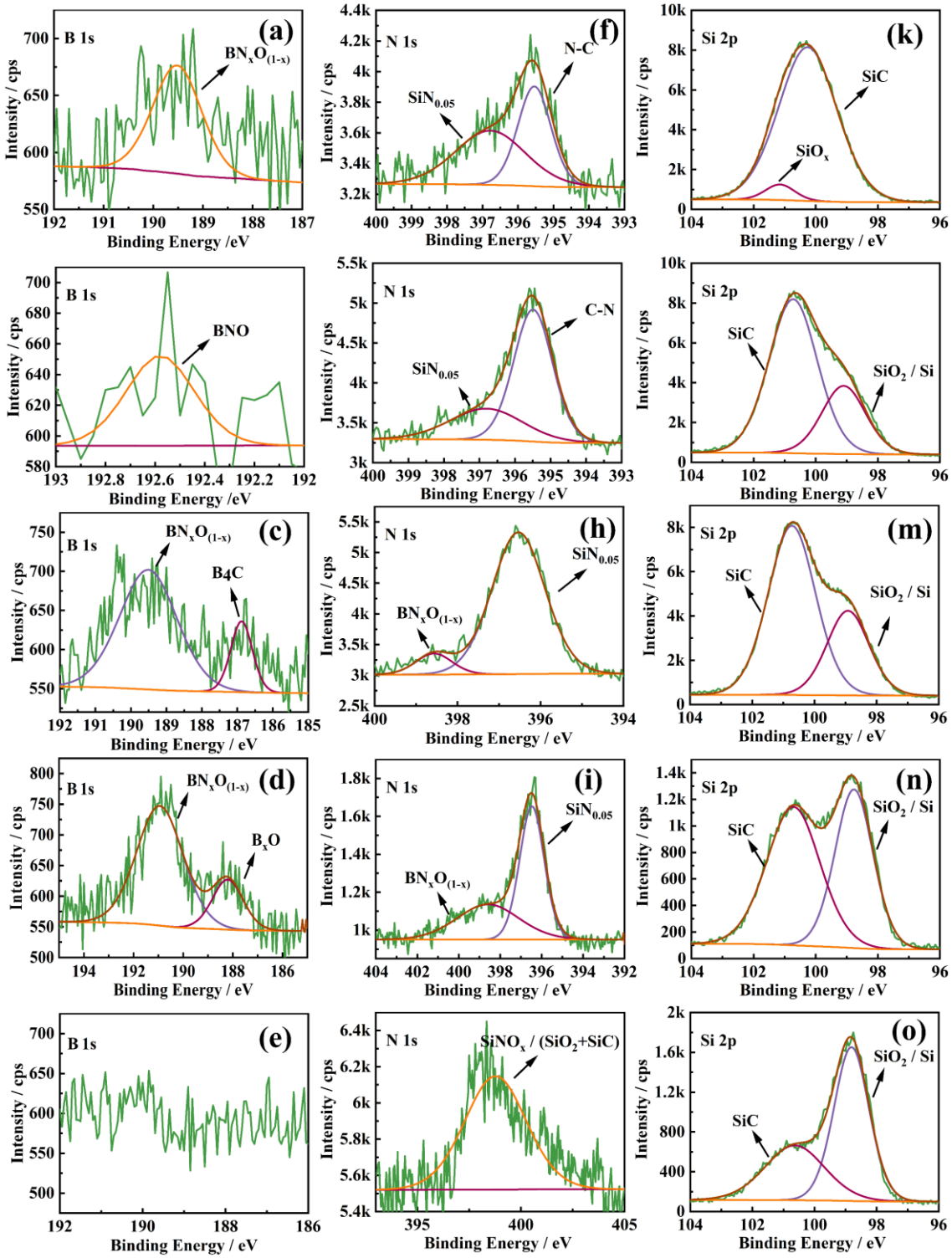

Figure 4 XPS spectra of B, N and Si elements after pyrolysis of SiBCN(O) ceramics at 1000 °C ((a), (f), (k)), 1200 °C ((b), (g), (l)), 1400 °C ((c), (h), (m)), 1600 °C ((d), (i), (n)) and 1800 °C ((e), (j), (o)).

Figure 5 shows HRTEM images and electron diffraction patterns of SiBCN(O) ceramics after pyrolysis at 1000 °C, 1200 °C, 1400 °C, 1600 °C and 1800 °C respectively.

The SiBCN(O) ceramics was amorphous before 1400 °C, which corresponds to the XRD results. After pyrolysis at 1400 °C and above, SiC crystallites could be observed. Because of the presence of B, the crystallization at 1400 °C was suppressed. However, the diffraction intensity grew higher with pyrolysis temperature, indicating more crystallization. A d-spacing of 0.252 nm from the TEM images can be assigned to the (111) plane of SiC, which corresponds to the PDF card of β-SiC crystalline. Figure 5(i)-(j) were the TEM images at 1800 °C. The HRTEM image shows a clear crystalline lattice. In addition, the diffraction spot has obvious elongated light rays. The amorphous regions are SiO_2, which could be verified by elemental analysis and XPS analysis.

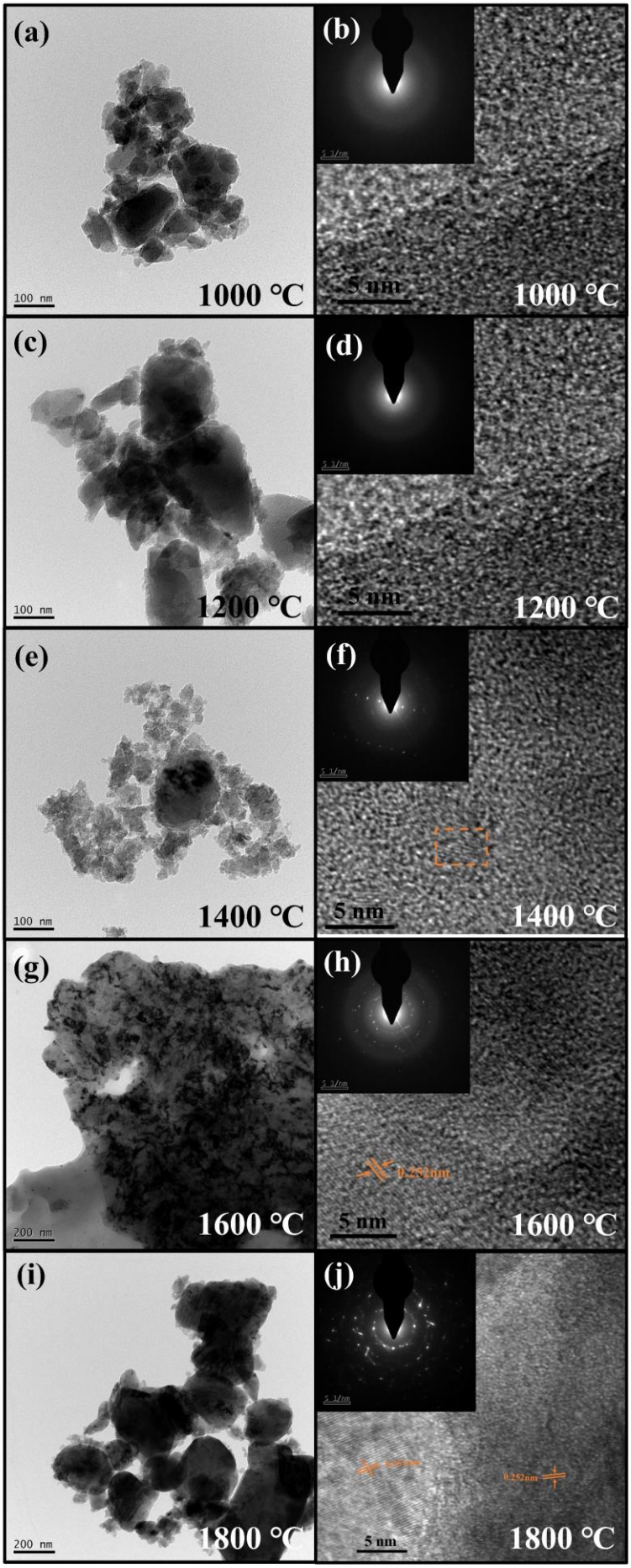
(a)
100 nm
1000 °C
(b)
5 nm
1000 °C
(c)
100 nm
1200 °C
(d)
5 nm
1200 °C
(e)
100 nm
1400 °C
(f)
5 nm
1400 °C
(g)
200 nm
1600 °C
(h)
0.251nm
5 nm
1600 °C
(i)
200 nm
1800 °C
(j)
0.252nm
5 nm
1800 °C

Figure 5 The TEM images of SiBCN(O) ceramics pyrolyzed at different temperatures.

Table 2 shows the chemical element composition of the pyrolyzed SiBCN(O) ceramics sintered at different temperatures. Compared with the CPBCSs precursor curing at 300 °C, the content of C element at 1000 °C decreased by 10 wt%, which could be attributed to the cleavage and escape of organic groups. Similar to C, N content also decreased because of escaping of nitrogen-containing molecules during pyrolysis. Most of the oxygen existed in the form of Si-O-, which could be proved by the peak at 1090 cm^{-1} in FTIR spectra. (Figure 3 (a)) If the pyrolysis temperature was 1600 °C, the content of O element decreased by about 10 wt%, which is attributed to carbothermal reaction.

Table 2 Chemical element composition of SiBCN(O) ceramics pyrolyzed at different temperatures

Temperatre / Samples	Element composition（wt%）						Empirical formula
	Si	B	C	O	N	H	
300 °C-SiBCN(O)3-1	33.05	1.37	32.90	20.23	3.80	8.65	$SiB_{0.11}C_{2.32}N_{0.23}O_{1.07}H_{7.34}$
300 °C-SiBCN(O)5-1	35.40	1.02	30.10	19.80	5.33	8.35	$SiB_{0.07}C_{1.99}N_{0.30}O_{0.98}H_{6.62}$
300 °C-SiBCN(O)10-1	44.30	0.63	24.50	20.22	2.80	7.55	$SiB_{0.04}C_{1.29}N_{0.13}O_{0.80}H_{4.87}$
1000 °C-SiBCN(O)3-1	50.01	0.92	18.79	27.34	2.95	-	$SiB_{0.02}C_{0.38}N_{0.06}O_{0.55}$
1000 °C-SiBCN(O)5-1	56.15	0.89	19.87	20.49	2.59	-	$SiB_{0.02}C_{0.35}N_{0.05}O_{0.36}$
1000 °C-SiBCN(O)10-1	49.00	0.10	20.68	25.87	3.46	-	$SiB_{0.02}C_{0.42}N_{0.07}O_{0.53}$
1200 °C-SiBCN(O)3-1	47.52	1.43	22.11	27.40	1.54	-	$SiB_{0.03}C_{0.47}N_{0.03}O_{0.58}$
1200 °C-SiBCN(O)5-1	50.37	0.91	20.74	25.88	2.12	-	$SiB_{0.02}C_{0.47}N_{0.04}O_{0.51}$
1200 °C-SiBCN(O)10-1	51.21	0.66	18.95	27.52	1.66	-	$SiB_{0.01}C_{0.41}N_{0.03}O_{0.54}$
1400 °C-SiBCN(O)3-1	47.77	2.47	23.21	25.06	1.49	-	$SiB_{0.02}C_{0.37}N_{0.03}O_{0.51}$
1400 °C-SiBCN(O)5-1	49.73	1.60	19.98	26.30	2.39	-	$SiB_{0.03}C_{0.47}N_{0.05}O_{0.53}$
1400 °C-SiBCN(O)10-1	53.20	0.82	21.37	22.73	1.88	-	$SiB_{0.05}C_{0.41}N_{0.04}O_{0.44}$

1600 °C-SiBCN(O)3-1	55.79	2.68	25.42	14.88	1.23	-	$SiB_{0.02}C_{0.44}N_{0.02}O_{0.26}$
1600 °C-SiBCN(O)5-1	58.16	1.72	22.85	15.69	1.59	-	$SiB_{0.03}C_{0.39}N_{0.03}O_{0.27}$
1600 °C-SiBCN(O)10-1	57.09	1.01	26.10	14.48	1.32	-	$SiB_{0.05}C_{0.47}N_{0.02}O_{0.26}$

3.3. Thermal stability of SiBCN(O) ceramics

To investigate the thermal stability of SiBCN(O) ceramics, thermal analysis of SiBCN(O) ceramics pyrolyzed at 1000 °C was performed in the air and argon atmosphere. (Figure 6) The SiBCN(O) ceramics showed a small loss at 1580 °C in argon while they showed no significant weight loss in air, demonstrating good thermal stability in both inert gas and air. The ceramic yields at 1600 °C were 98.32 wt%, 98.29 wt%, 95.72 wt% for the SiBCN(O)10-1, SiBCN(O)5-1, SiBCN(O)3-1 ceramics in argon, while the ceramic yields were 99.17%, 99.36% and 99.87% in air, respectively. In argon, the increased weight loss of ceramics at 1580°C is mainly due to the carbothermal reduction reaction and the cracking of Si-N compounds[41]. In air atmosphere, the oxidation behavior of BC units is similar to BN(C), which could be oxidized to produce B_2O_3 phase. B_2O_3 may be transformed into the liquid state at high temperature, covering the surface of ceramic and preventing further oxidation. B_2O_3 may react with glassy SiO_2 to form a stable borosilicate or SiO_2-B_2O_3 binary melt and the borosilicate glass can withstand up to 1600 °C. The dense borosilicate glass layer also inhibits further oxidation[13, 42]. Therefore, the char yield increased with boron content.

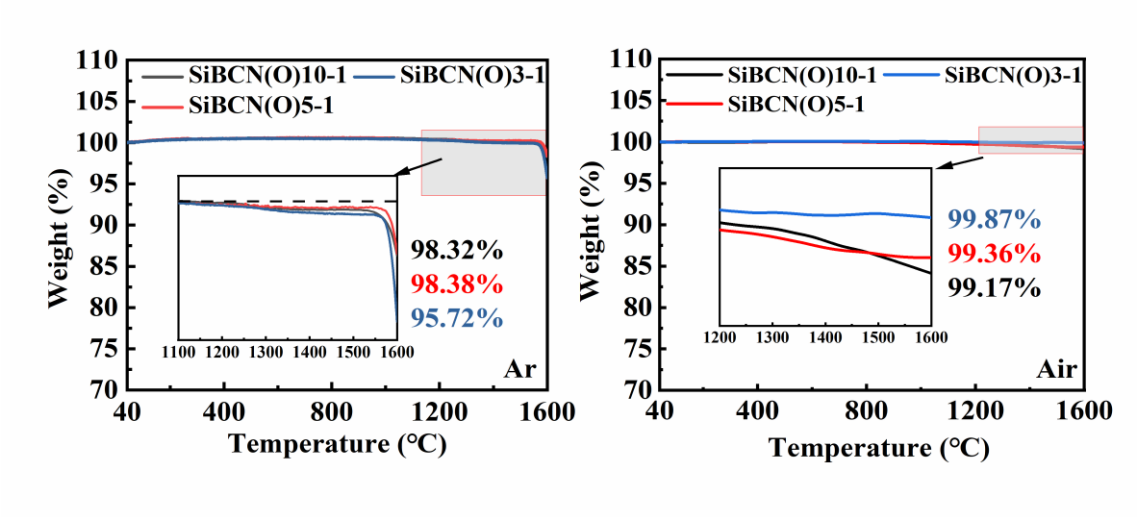

Figure 6 TG curves of SiBCN(O) ceramics in argon and air atmosphere.

4. Conclusion

In this work, we fabricated SiBCN(O) ceramics through pyrolysis of polyborosilazanes and investigated the microstructure evolution of them. The precursors were converted into amorphous ceramics when heated above 800 °C in argon. The two-component structure can adjust the boron content and provide different thermal oxygen properties. The SiBCN(O) ceramics remain amorphous till 1600 °C and the incorporation of boron suppressed the carbothermal reaction. The as-prepared SiBCN(O) ceramics showed good thermal stability in both argon and nitrogen, and no significant weight loss could be observed before 1600 °C. These new SiBCN(O) might be candidate for harsh environments where extreme service temperature is needed.

Acknowledgements

The authors gratefully acknowledge financial support by the Chinese Academy of Science and Ningbo 3315 plan (Grant No. 2018A-03-A). Dr. Ke Chen acknowledges

the financial support by National Natural Science Foundation of China (Grant No. 51902319).

References

[1] S. Yajima, J. Hayashi, M. Omori, Continuous Silicon Carbide Fiber of High Tensile Strength, Chem. Lett., 4 (1975) 931-934. https://doi.org/10.1246/cl.1975.931.

[2] S. Yajima, J. Hayashi, M. Omori, K. Okamura, Development of a Silicon-Carbide Fiber with High-Tensile Strength, Nature, 261 (1976) 683-685. https://doi.org/10.1038/261683a0.

[3] S. Yajima, J. Hayashi, K. Okamura, Pyrolysis of a Polyborodiphenylsiloxane, Nature, 266 (1977) 521-522. https://doi.org/10.1038/266521a0.

[4] M. Birot, J.P. Pillot, J. Dunogues, Comprehensive Chemistry of Polycarbosilanes, Polysilazanes, and Polycarbosilazanes as Precursors of Ceramics, Chem. Rev., 95 (1995) 1443-1477. https://doi.org/10.1021/cr00037a014.

[5] R.J. Corriu, Ceramics and Nanostructures from Molecular Precursors, Angew Chem Int Ed Engl, 39 (2000) 1376-1398. https://doi.org/10.1002/(sici)1521-3773(20000417)39:8<1376::aid-anie1376>3.0.co;2-s.

[6] E. Kroke, Y.L. Li, C. Konetschny, E. Lecomte, C. Fasel, R. Riedel, Silazane derived ceramics and related materials, Materials Science & Engineering R-Reports, 26 (2000) 97-199. https://doi.org/10.1016/S0927-796x(00)00008-5.

[7] X. Li, X.L. Pei, X.Q. Zhong, G.M. Mo, L. He, Z.R. Huang, Q. Huang, Highly effective free-radical-catalyzed curing of hyperbranched polycarbosilane for near stoichiometric SiC ceramics, J. Am. Ceram. Soc., 102 (2019) 1041-1048. https://doi.org/10.1111/jace.15966.

[8] Y.S. Jang, C. Zollfrank, M. Jank, P. Greil, Fabrication of Silicon Carbide Micropillar Arrays from Polycarbosilanes, J. Am. Ceram. Soc., 93 (2010) 3929-3934. https://doi.org/10.1111/j.1551-2916.2010.03978.x.

[9] J. Wu, Y. Li, L. Chen, Z. Zhang, D. Wang, C. Xu, Simple Fabrication of Micro/Nano-Porous SiOC Foam from Polysiloxane, J. Mater. Chem., 22 (2012) 6542-6545. https://doi.org/10.1039/C2JM16840E.

[10] Q. Yuan, Z.F. Chai, Z.R. Huang, Q. Huang, A new precursor of liquid and curable polysiloxane for highly cost-efficient SiOC-based composites, Ceram. Int., 45 (2018) 7044-7048. https://doi.org/10.1016/j.ceramint.2018.12.206.

[11] O. Flores, R.K. Bordia, D. Nestler, W. Krenkel, G. Motz, Ceramic Fibers Based on SiC and SiCN Systems: Current Research, Development, and Commercial Status, Adv. Eng. Mater., 16 (2014) 621-636. https://doi.org/10.1002/adem.201400069.

[12] B. Mu, T. Liu, W. Tian, Long-Chain Hyperbranched Polymers: Synthesis, Properties, and Applications, Macromol Rapid Commun, 40 (2019) e1800471. https://doi.org/10.1002/marc.201800471.

[13] D.X. Li, Z.H. Yang, D.C. Jia, X.M. Duan, D.L. Cai, S.J. Wang, J.K. Yuan, Y. Zhou, D.L. Yu, Y.J. Tian, High-temperature oxidation resistance of dense amorphous boron-rich SiBCN monoliths, Corros. Sci., 157 (2019) 312-323. https://doi.org/10.1016/j.corsci.2019.06.001.

[14] A. Viard, D. Fonblanc, M. Schmidt, A. Lale, C. Salameh, A. Soleilhavoup, M. Wynn, P. Champagne, S. Cerneaux, F. Babonneau, G. Chollon, F. Rossignol, C. Gervais, S. Bernard, Molecular Chemistry and Engineering of Boron-Modified Polyorganosilazanes as New Processable and Functional SiBCN

Precursors, Chemistry (Easton), 23 (2017) 9076-9090. https://doi.org/10.1002/chem.201700623.
[15] M.A. Schiavon, N.A. Armelin, I.V.P. Yoshida, Novel poly(borosiloxane) precursors to amorphous SiBCO ceramics, Mater. Chem. Phys., 112 (2008) 1047-1054. https://doi.org/10.1016/j.matchemphys.2008.07.041.
[16] X. Wang, J. Shi, H. Wang, Preparation, properties, and structural evolution of a novel polyborosilazane adhesive, temperature-resistant to 1600 degrees C for joining SiC ceramics, J. Alloys Compd., 772 (2019) 912-919. https://doi.org/10.1016/j.jallcom.2018.09.110.
[17] A. Viard, P. Miele, S. Bernard, Polymer-derived ceramics route toward SiCN and SiBCN fibers: from chemistry of polycarbosilazanes to the design and characterization of ceramic fibers, J. Ceram. Soc. Jpn., 124 (2016) 967-980. https://doi.org/10.2109/jcersj2.16124.
[18] R. Riedel, H.J. Kleebe, H. Schonfelder, F. Aldinger, A Covalent Micro Nanocomposite Resistant To High-Temperature Oxidation, Nature, 374 (1995) 526-528. https://doi.org/10.1038/374526a0.
[19] M. Weinmann, R. Haug, J. Bill, F. Aldinger, J. Schuhmacher, K. Muller, Boron-containing polysilylcarbodi-imides: a new class of molecular precursors for Si-B-C-N ceramics, J. Organomet. Chem., 541 (1997) 345-353. https://doi.org/10.1016/s0022-328x(97)00085-5.
[20] A. Muller, P. Gerstel, M. Weinmann, J. Bill, F. Aldinger, Correlation of boron content and high temperature stability in Si-B-C-N ceramics, J. Eur. Ceram. Soc., 20 (2000) 2655-2659. https://doi.org/10.1016/s0955-2219(00)00131-x.
[21] Z. Yu, C. Zhou, R. Li, L. Yang, S. Li, H. Xia, Synthesis and ceramic conversion of a novel processible polyboronsilazane precursor to SiBCN ceramic, Ceram. Int., 38 (2012) 4635-4643. https://doi.org/10.1016/j.ceramint.2012.02.045.
[22] A. Müller, P. Gerstel, M. Weinmann, J. Bill, F. Aldinger, Correlation of boron content and high temperature stability in Si–B–C–N ceramics, J. Eur. Ceram. Soc., 20 (2000) 2655-2659. https://doi.org/10.1016/s0955-2219(00)00131-x.
[23] D. Li, Z. Yang, D. Jia, D. Cai, S. Wang, Q. Chen, Y. Zhou, D. Yu, Y. Tian, Boron-dependent microstructural evolution, thermal stability, and crystallization of mechanical alloying derived SiBCN, J. Am. Ceram. Soc., 101 (2018) 3205-3221. https://doi.org/10.1111/jace.15428.
[24] B. Wang, K. Chen, T. Li, X. Sun, M. Liu, L. Yang, X. Hu, J. Xu, L. He, Q. Huang, L. Jiang, Y. Song, High-Temperature Resistant Polyborosilazanes with Tailored Structures, Polymers (Basel), 13 (2021) 467. https://doi.org/10.3390/polym13030467.
[25] W.-H. Li, J. Wang, Z.-F. Xie, H. Wang, A novel polyborosilazane for high-temperature amorphous Si–B–N–C ceramic fibres, Ceram. Int., 38 (2012) 6321-6326. https://doi.org/10.1016/j.ceramint.2012.05.001.
[26] Y. Tang, J. Wang, X.-D. Li, H. Wang, W.-H. Li, X.-Z. Wang, Preceramic polymer for Si B N C fiber via one-step condensation of silane, BCl3, and silazane, J. Appl. Polym. Sci., 110 (2008) 921-928. https://doi.org/10.1002/app.28679.
[27] Y.-L. Li, E. Kroke, R. Riedel, C. Fasel, C. Gervais, F. Babonneau, Thermal cross-linking and pyrolytic conversion of poly(ureamethylvinyl)silazanes to silicon-based ceramics, Appl. Organomet. Chem., 15 (2001) 820-832. https://doi.org/10.1002/aoc.236.
[28] V. Belot, R.J.P. Corriu, D. Leclercq, P.H. Mutin, A. Vioux, Organosilicon Gels Containing Silicon Silicon Bonds, Precursors To Novel Silicon Oxycarbide Compositions, J. Non-Cryst. Solids, 144 (1992) 287-297. https://doi.org/10.1016/S0022-3093(05)80412-0.
[29] T. Shimoo, K. Okamura, T. Akizuki, M. Takemura, Preparation of SiC-C composite fibre by carbothermic reduction of silica, Journal of Materials Science, 30 (1995) 3387-3394. https://doi.org/10.1007/BF00349884.

[30] J. Latournerie, P. Dempsey, D. Hourlier-Bahloul, J.-P. Bonnet, Silicon Oxycarbide Glasses: Part 1-Thermochemical Stability, J. Am. Ceram. Soc., 89 (2006) 1485-1491. https://doi.org/10.1111/j.1551-2916.2005.00869.x.
[31] B.J. Tang, Y. Zhang, S.J. Hu, B. Feng, A dense amorphous SiBCN(O) ceramic prepared by simultaneous pyrolysis of organics and inorganics, Ceram. Int., 42 (2016) 5238-5244. https://doi.org/10.1016/j.ceramint.2015.12.050.
[32] W. He, L. Chen, T. Xu, F. Peng, Borazine-type single source precursor with vinyl to SiBCN ceramic, J. Ceram. Soc. Jpn., 126 (2018) 253-259. https://doi.org/10.2109/jcersj2.17236.
[33] A.B. Kousaalya, R. Kumar, S. Packirisamy, Characterization of free carbon in the as-thermolyzed Si-B-C-N ceramic from a polyorganoborosilazane precursor, Journal of Advanced Ceramics, 2 (2013) 325-332. https://doi.org/10.1007/s40145-013-0079-4.
[34] K. Goehlert, G. Irmer, L. Michalowsky, J. Monecke, Polytype analysis of SiC Powders by Raman spectroscopy, J. Mol. Struct., 219 (1990) 135-140. https://doi.org/10.1016/0022-2860(90)80045-L.
[35] N. Liu, A. Steele, L.R. Nittler, R.M. Stroud, B.T. De Gregorio, C.M.O.D. Alexander, J. Wang, Coordinated EDX and micro-Raman analysis of presolar silicon carbide: A novel, nondestructive method to identify rare subgroup SiC, Meteoritics & Planetary Science, 52 (2017) 2550-2569. https://doi.org/10.1111/maps.12954.
[36] M. Yan, W. Song, C. Zhao-hui, Raman spectroscopy studies of the high-temperature evolution of the free carbon phase in polycarbosilane derived SiC ceramics, Ceram. Int., 36 (2010) 2455-2459. https://doi.org/10.1016/j.ceramint.2010.08.003.
[37] N. Shirahata, K. Kijima, X. Ma, Y. Ikuhara, Thermal Change of Unstable Stacking Faults in β-SiC, Japanese Journal of Applied Physics, 40 (2001) 3969-3974. https://doi.org/10.1143/jjap.40.3969.
[38] H.P. Iwata, U. Lindefelt, S. Öberg, P.R. Briddon, Stacking faults in silicon carbide, Physica B: Condensed Matter, 340-342 (2003) 165-170. https://doi.org/10.1016/j.physb.2003.09.045.
[39] D. Li, Z. Yang, D. Jia, X. Duan, P. He, Y. Zhou, Ablation behavior of graphene reinforced SiBCN ceramics in an oxyacetylene combustion flame, Corros. Sci., 100 (2015) 85-100. https://doi.org/10.1016/j.corsci.2015.07.006.
[40] D. Li, Z. Yang, D. Jia, S. Wang, X. Duan, Q. Zhu, Y. Miao, J. Rao, Y. Zhou, High-temperature oxidation behavior of dense SiBCN monoliths: Carbon-content dependent oxidation structure, kinetics and mechanisms, Corros. Sci., 124 (2017) 103-120. https://doi.org/10.1016/j.corsci.2017.05.013.
[41] S. Wada, Control of instability of Si3N4 during pressureless sintering, J. Ceram. Soc. Jpn., 109 (2001) 803-808. https://doi.org/10.2109/jcersj.109.1274_803.
[42] X. Guo, D. Wang, Z. Guo, Z.B. Zhang, M.Z. Cui, C.H. Xu, SiBCN-precursor-derived gradient oxidation protective ceramic coating for C/C composites, Surf Coat Technol, 350 (2018) 101-109. https://doi.org/10.1016/j.surfcoat.2018.06.091.

Figure Captions

Figure 1 Optical picture of (a) CPBCS precursor; (b) CPBCS precursor after cured at 300 °C; (c) CPBCS precursor after pyrolysis at 1200 °C; (d) SEM of derived ceramics at 1200 °C.

Figure 2 (a)FT-IR spectrum of CPBCS 5-1 samples treated at different temperatures; (b) TG-MS curves of CPBCS 5-1 in argon

Figure 3 (a) The FT-IR spectra of SiBCN(O) ceramics pyrolyzed from 1000 °C to 1800°C in argon; (b) Raman spectra of SiBCN(O) ceramics heated from 1000 °C to 1800°C in argon.; (c) XRD patterns of SiBCN(O) ceramic pyrolyzed at different high temperature.

Figure 4 XPS spectra of B, N and Si elements after pyrolysis of SiBCN(O) ceramics at 1000 °C ((a), (f), (k)), 1200 °C ((b), (g), (l)), 1400 °C ((c), (h), (m)), 1600 °C ((d), (i), (n)) and 1800 °C ((e), (j), (o)).

Figure 5 The TEM images of SiBCN(O) ceramics pyrolyzed at different temperatures.

Figure 6 TG curves of SiBCN(O) ceramics in argon and air atmosphere.